

Universality of the glassy transitions in the two-dimensional $\pm J$ Ising model

Francesco Parisen Toldin*

Max-Planck-Institut für Metallforschung, Heisenbergstrasse 3, D-70569 Stuttgart, Germany
and Institut für Theoretische und Angewandte Physik, Universität Stuttgart, Pfaffenwaldring 57, D-70569 Stuttgart, Germany

Andrea Pelissetto†

Dipartimento di Fisica, dell'Università di Roma "La Sapienza" and INFN, Piazzale Aldo Moro 2, I-00185 Roma, Italy

Ettore Vicari‡

Dipartimento di Fisica, dell'Università di Pisa and INFN, Largo Pontecorvo 3, I-56127 Pisa, Italy

(Received 31 May 2010; published 9 August 2010)

We investigate the zero-temperature glassy transitions in the square-lattice $\pm J$ Ising model, with bond distribution $P(J_{xy}) = p\delta(J_{xy} - J) + (1-p)\delta(J_{xy} + J)$; $p=1$ and $p=1/2$ correspond to the pure Ising model and to the Ising spin glass with symmetric bimodal distribution, respectively. We present finite-temperature Monte Carlo simulations at $p=4/5$, which is close to the low-temperature paramagnetic-ferromagnetic transition line located at $p \approx 0.89$, and at $p=1/2$. Their comparison provides a strong evidence that the glassy critical behavior that occurs for $1-p_0 < p < p_0$, $p_0 \approx 0.897$, is universal, i.e., independent of p . Moreover, we show that glassy and magnetic modes are not coupled at the multicritical zero-temperature point where the paramagnetic-ferromagnetic transition line and the $T=0$ glassy transition line meet. On the theoretical side we discuss the validity of finite-size scaling in glassy systems with a zero-temperature transition and a discrete Hamiltonian spectrum. Because of a freezing phenomenon which occurs in a finite volume at sufficiently low temperatures, the standard finite-size scaling limit in terms of $TL^{1/\nu}$ does not exist; the renormalization-group invariant quantity ξ/L should be used instead as basic variable.

DOI: [10.1103/PhysRevE.82.021106](https://doi.org/10.1103/PhysRevE.82.021106)

PACS number(s): 64.60.F-, 75.10.Nr, 75.50.Lk, 75.40.Mg

I. INTRODUCTION

The $\pm J$ Ising model [1] is a standard theoretical laboratory to study the effects of quenched disorder and frustration on the critical behavior of spin systems. We consider the two-dimensional (2D) $\pm J$ Ising model defined on a square lattice by the Hamiltonian

$$\mathcal{H} = - \sum_{\langle xy \rangle} J_{xy} \sigma_x \sigma_y, \quad (1)$$

where $\sigma_x = \pm 1$, the sum is over all pairs of lattice nearest-neighbor sites, and the exchange interactions J_{xy} are uncorrelated quenched random variables, taking values $\pm J$ with probability distribution

$$P(J_{xy}) = p\delta(J_{xy} - J) + (1-p)\delta(J_{xy} + J). \quad (2)$$

For $p=1$ we recover the standard Ising model, while for $p=1/2$ we obtain the so-called bimodal Ising glass model. For $p \neq 1/2$, the disorder average of the couplings is given by $[J_{xy}] = J(2p-1) \neq 0$ and ferromagnetic (or antiferromagnetic) configurations are energetically favored. Note that its thermodynamic behavior is symmetric under $p \rightarrow 1-p$. In the following we set $J=1$ without loss of generality.

The 2D $\pm J$ Ising model has been extensively investigated; see, e.g., Refs. [2–4] for recent reviews. As sketched in Fig. 1, at finite temperature it presents a paramagnetic and

a ferromagnetic phase. They are separated by a transition line, which starts at the pure Ising transition point, at $p=1$ and $T_{Is} = 2/\ln(1+\sqrt{2}) = 2.269\,19\dots$, and ends at the disorder-driven ferromagnetic $T=0$ transition, at [5,6] $p_0 \approx 0.897$. The point where this transition line meets the so-called Nishimori (N) line [2,7,8], at [4] $T_M = 0.9527(1)$ and $p_M = 0.890\,83(3)$ (see also Refs. [9,10] for analytical estimates of T_M, p_M) is a multicritical point (MNP) [11,12]. The MNP divides the paramagnetic-ferromagnetic (PF) transition line in two parts. The PF transition line from the Ising point at $p=1$ to the MNP is controlled by the Ising fixed point. Here disorder gives only rise to (universal) logarithmic corrections to the standard Ising critical behavior; see, e.g., Ref. [13] and ref-

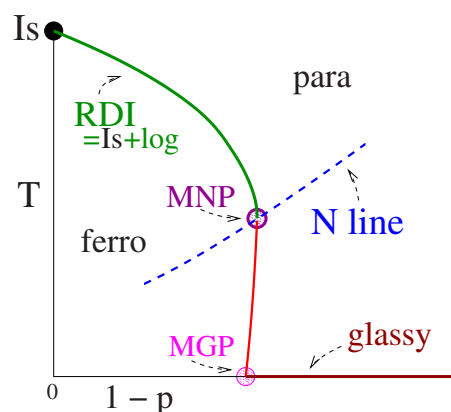


FIG. 1. (Color online) Phase diagram of the square-lattice $\pm J$ Ising model in the T - p plane. The phase diagram is symmetric under $p \rightarrow 1-p$.

*parisen@mf.mpg.de

†andrea.pelissetto@roma1.infn.it

‡vicari@df.unipi.it

erences therein. The slightly reentrant low-temperature PF transition for $T < T_M$ belongs instead to a different strong-disorder (SDI) universality class [4,14–16].

Several studies [17,18,20–30] have discussed the possible existence of a glassy transition, considering in most of the cases models with symmetric disorder distributions such that $[J_{xy}] = 0$. At variance with the three-dimensional case, no finite-temperature glassy phase occurs and a critical behavior is only observed at $T=0$. Moreover, recent results for the bimodal Ising model [27–30] have provided compelling evidence that the bimodal Ising model and other models with symmetric continuous disorder distributions, for instance the Gaussian distribution, undergo a zero-temperature glassy transition in the same universality class. In all cases, for $T \rightarrow 0$ the correlation length increases as $T^{-\nu}$ with [31] $\nu \approx 3.55$. Even though the critical behavior in the thermodynamic limit (i.e., if one takes $L \rightarrow \infty$ before $T \rightarrow 0$) is the same [27], for small values of the temperature and in finite volume the bimodal Ising glass model, and in general any model with a discrete Hamiltonian spectrum, does not behave as models with continuous disorder distributions. In particular, as we shall see, in the bimodal Ising glass model one cannot observe the standard finite-size scaling (FSS) limit in terms of the scaling variable $TL^{1/\nu}$. An appropriate variable is instead the renormalization-group (RG) invariant quantity ξ/L .

In the case of the $2D \pm J$ Ising model, a natural scenario is that a zero-temperature glassy transition occurs for any p in the range $1-p_0 < p < p_0$, and that the glassy critical behavior is independent of p . This implies that a nonzero $[J_{xy}]$ is irrelevant for the critical behavior, as found in mean-field models [32] and in the $3D \pm J$ Ising model [33].

In this paper, which completes a series of papers [4,12,13] devoted to the study of the phase diagram and critical behavior of the $2D \pm J$ Ising model, we investigate the glassy behavior for $1-p_0 < p < p_0$. For this purpose, we present Monte Carlo (MC) simulations at $p=4/5$, which is relatively close to the low-temperature PF line ($p_0 \approx p_{MNP} \approx 0.89$), and at $p=1/2$, up to lattice sizes $L=64$ and for $T \gtrsim 0.1$. As we shall see, our results provide a strong evidence of the universality of the glassy zero-temperature critical behavior and thus provide strong support to the scenario of a universal glassy critical line for $T=0$ and $1-p_0 < p < p_0$. Moreover, we provide evidence that the magnetic and glassy behaviors at the $T=0$ multicritical glassy point (MGP), where the low-temperature PF and the $T=0$ glassy transition lines meet, at $p_0 \approx 0.897$, see Fig. 1, are decoupled. Finally, we discuss the critical behavior of the overlap quantities along the PF line that connects the MNP to the $T=0$ MGP: we observe an apparently T -dependent critical behavior.

The paper is organized as follows. In Sec. II, we define the quantities we have considered in the MC simulations. In Sec. III, we discuss the behavior at the $T=0$ glassy transition. In particular, we discuss the freezing phenomenon observed in a finite volume at very small temperatures due to the discreteness of the Hamiltonian spectrum, the universality of the glassy critical behavior, and the critical behavior of the overlap susceptibility. In Sec. IV, we discuss the critical behavior of the overlap correlations along the low-temperature paramagnetic-ferromagnetic transition line, below the MNP. Finally, In Sec. V, we draw our conclusions.

II. DEFINITIONS

The critical modes at the glassy transition are those related to the overlap variable $q_x \equiv \sigma_x^{(1)} \sigma_x^{(2)}$, where the spins $\sigma_x^{(i)}$ belong to two independent replicas with the same disorder realization $\{J_{xy}\}$. In our MC simulations we measure the overlap susceptibility χ and the second-moment correlation length ξ defined from the correlation function $G_o(x) \equiv [\langle q_0 q_x \rangle] = [\langle \sigma_0 \sigma_x \rangle^2]$, where the angular and the square brackets indicate the thermal average and the quenched average over disorder, respectively. We define $\chi \equiv \Sigma_x G_o(x)$ and

$$\xi^2 \equiv \frac{1}{4 \sin^2(p_{\min}/2)} \frac{\tilde{G}_o(0) - \tilde{G}_o(p)}{\tilde{G}_o(p)}, \quad (3)$$

where $p = (p_{\min}, 0)$, $p_{\min} \equiv 2\pi/L$, and $\tilde{G}_o(q)$ is the Fourier transform of $G_o(x)$. We also consider some quantities that are invariant under RG transformations in the critical limit, which we call phenomenological couplings. We consider the ratio ξ/L and the quartic cumulants

$$U_4 \equiv \frac{[\rho_4]}{[\rho_2]^2}, \quad U_{22} \equiv \frac{[\rho_2^2] - [\rho_2]^2}{[\rho_2]^2}, \quad (4)$$

where $\rho_k \equiv \langle (\Sigma_x q_x)^k \rangle$.

In the case of a $T=0$ transition with a nondegenerate ground state, as expected in the 2D Ising glass model with a Gaussian disorder distribution, we have $\chi \sim \xi^2$ for $T=0$, hence the corresponding overlap-susceptibility exponent η vanishes, $\eta=0$, and

$$U_4 \rightarrow 1, \quad U_{22} \rightarrow 0 \quad (5)$$

for $T \rightarrow 0$. In particular, $U_{22} \rightarrow 0$ indicates the self-averaging of the ground-state distribution, as already suggested by the results of Ref. [34]. Moreover, since $\eta=0$, it is natural to conjecture that the two-point overlap function becomes essentially Gaussian in the limit $T \rightarrow 0$. If this occurs, we also have $\xi/L \rightarrow \infty$. As we shall see, the results for the $\pm J$ Ising model are consistent with these predictions.

We also consider magnetic quantities. We define the magnetic susceptibility χ_m and the second-moment correlation length ξ_m in terms of the magnetic two-point function

$$G_m(x) \equiv [\langle \sigma_0 \sigma_x \rangle]. \quad (6)$$

For symmetric disorder distributions we have [35] $\chi_m = 1$ and $\xi_m = 0$ for any T . For other values of p , we expect them to converge to a finite nonuniversal value. We also consider the four-point magnetic susceptibility χ_{4m} defined by

$$\chi_{4m} \equiv [\mu_4 - 3\mu_2^2]/L^2, \quad (7)$$

$$\mu_k \equiv \left\langle \left(\sum_x \sigma_x \right)^k \right\rangle. \quad (8)$$

For symmetric disorder distributions we have [35]

$$\chi_{4m} = 4 - 6\chi. \quad (9)$$

Assuming universality we expect $\chi_{4m} \sim \chi$ also for nonsymmetric disorder distributions, i.e., for any $p \neq 1/2$.

III. RESULTS AT THE GLASSY TRANSITIONS

We perform MC simulations of the square-lattice $\pm J$ Ising model with periodic boundary conditions for $p=4/5$ and $p=1/2$ and for several values of the lattice size L , with $8 \leq L \leq 64$. We employ the Metropolis algorithm, the random-exchange method [36], and multispin coding. Furthermore, for the largest lattices ($L \geq 32$) we use the cluster algorithm described in Ref. [18]. For each lattice size we collect data in the range [19] $T_{\min} \leq T \leq T_{\max}$, with $1.1 \leq T_{\max} \leq 1.4$. At $p=4/5$ we take $T_{\min}=0.1$ for $L \leq 32$, $T_{\min}=1/2.6 \approx 0.38$ for $L=48$, $T_{\min}=1/2.7 \approx 0.37$ for $L=64$. At $p=1/2$, we take $T_{\min}=0.1$ for $L \leq 16$ and $T_{\min}=1/3.3$ for $24 \leq L \leq 64$. Typically, we consider 10^4 disorder samples for each T and p . In a few cases, we consider 10^5 disorder samples. In the following, we first discuss the freezing regime, which occurs for sufficiently low temperatures in any finite system, then we provide strong numerical evidence of the universality of the glassy transition by considering the FSS behavior of the phenomenological couplings ξ/L , U_4 , and U_{22} , and finally discuss the behavior of the overlap susceptibility and of the magnetic quantities.

A. Frozen regime

In Figs. 2 and 3 we show the MC estimates of ξ/L , U_4 , and U_{22} . We note that the data corresponding to different lattice sizes cross each other around $T \approx 0.3$ and are mostly independent of T for $T \leq 0.3$. Similar results for U_4 using the bimodal distribution were also reported in Ref. [18]. Usually, a crossing point corresponds to a transition point. Instead, in the present case in which the disorder variables are discrete, the crossing is due to a nonuniversal phenomenon which is related to the discreteness of the Hamiltonian spectrum [27,28].

To review the argument, let us consider the states corresponding to the two lowest energy values for a given lattice size L . Their energies differ by $\Delta \equiv E_1 - E_0 = 4$ and their degeneracies are given by $N_0(L)$ and $N_1(L)$, respectively. Numerical studies [23] have shown that $\ln N_1/N_0 \approx 4 \ln L$. At sufficiently low temperatures only the states with the lowest energy contribute to the thermodynamics. This occurs when $N_0(L) \gg N_1(L)e^{-\Delta/T}$, i.e., for

$$T \ll \frac{\Delta}{\ln[N_1(L)/N_0(L)]} \sim \frac{1}{\ln L}. \quad (10)$$

In this regime the observed behavior is independent of T . In the opposite limit, i.e., when $N_0(L) \ll N_1(L)e^{-\Delta/T}$, the presence of the gap is negligible and the system is expected to have the same behavior as models with continuous distributions. The crossover from one regime to the other occurs at an L -dependent freezing temperature $T_f(L)$ which scales as $1/\ln L$. It is natural to define $T_f(L)$ by requiring $N_0(L) = N_1(L)e^{-\Delta/T_f}$, but this definition is somewhat impractical. In practice, $T_f(L)$ can be estimated from the data by identifying it with the temperature that marks the onset of the T -independent behavior of the different observables. For $p=4/5$, the estimates of ξ/L and U_4 reported in Fig. 2 allow us to estimate $T_f(L) \approx 0.41, 0.36, 0.32$, and 0.28 for $L=8, 12$,

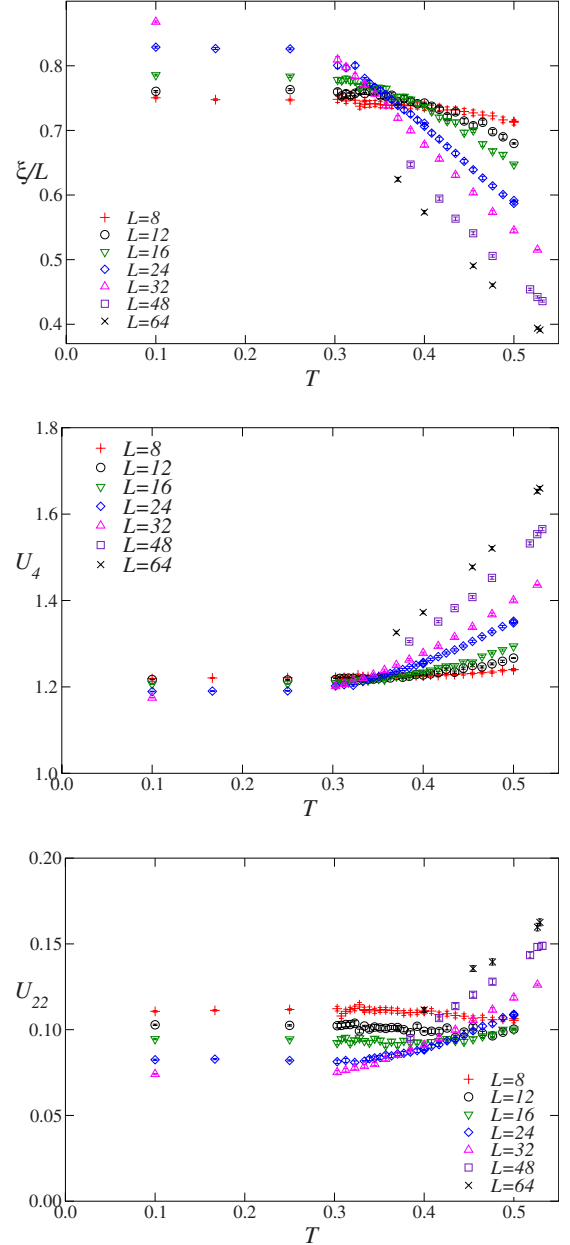


FIG. 2. (Color online) Phenomenological couplings ξ/L , U_4 , and U_{22} versus T at $p=4/5$.

16, and 24, respectively. Slightly larger results are obtained by using U_{22} . The estimates of $T_f(L)$ for $p=1/2$ are close to those obtained for $p=4/5$, showing that $T_f(L)$ is little dependent on p . Consistently with the above-reported argument, the freezing temperature $T_f(L)$ approximately decreases as $1/\ln L$, see Fig. 4. A fit to $c/\ln L$ gives $c \approx 0.9$. In the frozen region the estimates of the phenomenological couplings should be very close to the corresponding $T=0$ estimates, since they are essentially determined by the lowest-energy configurations. The data are consistent with this prediction. Indeed, see Fig. 4, for both $p=4/5$ and $p=1/2$, U_4 and U_{22} below T_f slowly approach the values $U_{22}=0$ and $U_4=1$, respectively, for $L \rightarrow \infty$. In particular, U_{22} apparently vanishes as $U_{22} \sim 1/\ln L$. Below T_f the ratio ξ/L increases as L , see Fig. 5, indicating that $\xi \sim L^2$ at $T=0$. These results imply

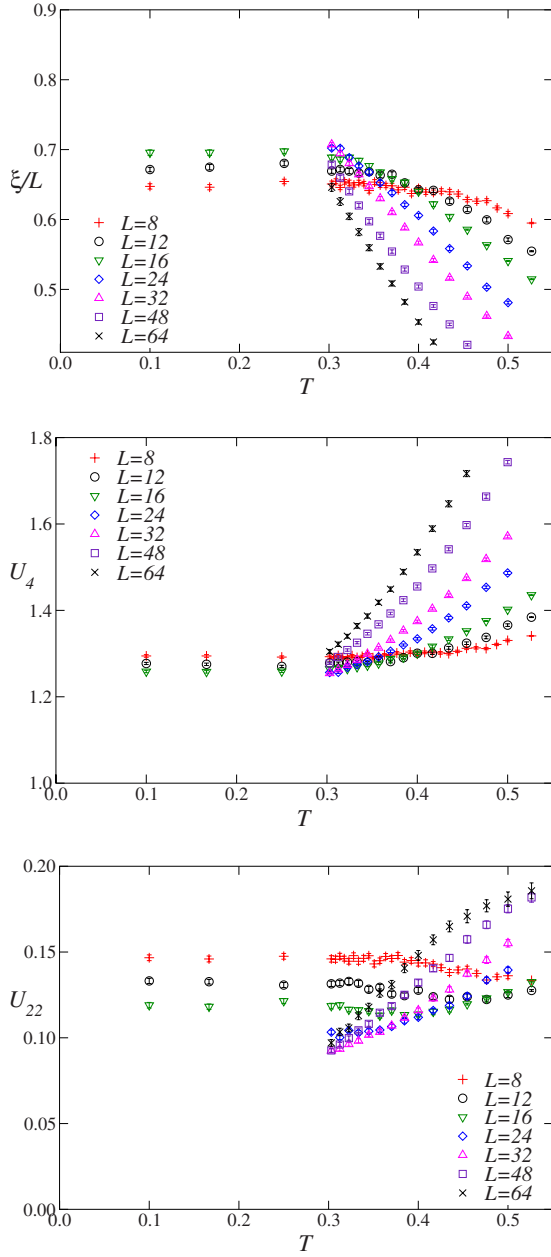


FIG. 3. (Color online) Phenomenological couplings ξ/L , U_4 , and U_{22} versus T at $p=1/2$.

that, at $T=0$, the large- L limit of the phenomenological couplings is identical to that observed in models with continuous distributions; in this case, as we discussed before, we predict $U_{22} \rightarrow 0$, $U_4 \rightarrow 1$, and $\xi/L \rightarrow \infty$. This equality should not be taken as an obvious fact. For instance, the stiffness exponent is different in the two cases.

B. Finite-size scaling in the presence of freezing

The presence of freezing for $T < T_f(L)$ makes the study of the $T=0$ glassy critical behavior quite hard. Indeed, in order to observe the glassy critical behavior in Ising glass models with a discrete Hamiltonian spectrum, one must approach $T=0$ by keeping $T \gg T_f(L)$ for each lattice size. This makes a

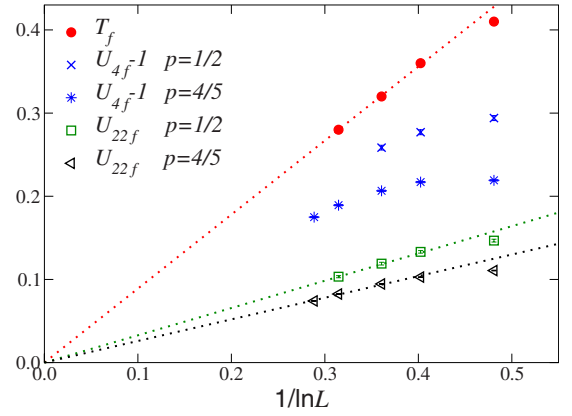


FIG. 4. (Color online) Freezing temperature $T_f(L)$ as estimated from the onset of the T -independent behavior for $T \rightarrow 0$, and estimates of U_{22} and U_4 in the frozen region (we indicate them by U_{4f} and U_{22f}). Results for $8 \leq L \leq 32$ and at the temperature $T=0.1$, which is well within the frozen region for the lattice sizes considered. The dotted lines are drawn to guide the eye.

standard FSS analysis impossible. Indeed, in the FSS limit a RG invariant quantity R should scale as

$$R = f_R(TL^{1/\nu}). \quad (11)$$

The condition $T \gg T_f(L)$ implies that this scaling behavior can only be observed for

$$TL^{1/\nu} \gg T_f(L)L^{1/\nu} \sim \frac{L^{1/\nu}}{\ln L}. \quad (12)$$

For $L \rightarrow \infty$, the ratio $L^{1/\nu}/\ln L$ diverges and thus this makes the range of values of $TL^{1/\nu}$ which are accessible smaller and smaller as L increases. This implies that the standard FSS limit, $T \rightarrow 0$, $L \rightarrow \infty$ at fixed $TL^{1/\nu}$ does not exist. However, as we shall now discuss, one can still study FSS if one uses the ratio ξ/L as basic FSS variable, i.e., if one considers the scaling form

$$R = g_R(\xi/L). \quad (13)$$

Usually, expressions Eqs. (11) and (13) are equivalent. This is not the case here: only the FSS scaling form Eq. (13) can

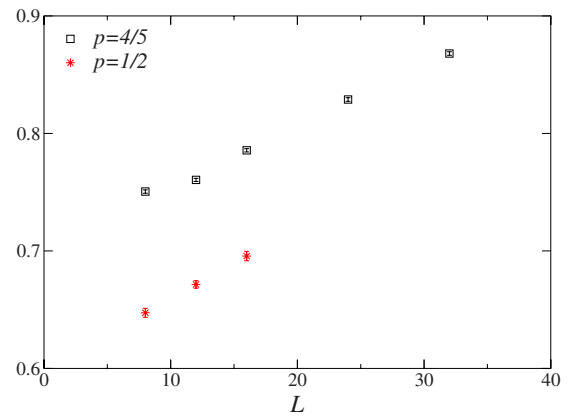


FIG. 5. (Color online) Estimates of ξ_f/L , where ξ_f is the value of ξ in the frozen region.

hold in the presence of freezing. As is clear from Figs. 2 and 3, the ratio ξ/L at fixed L increases as T decreases. Hence, the condition $T \gg T_f(L)$ translates into

$$\frac{\xi}{L} \ll \frac{\xi_f}{L}, \quad (14)$$

where ξ_f is the value of ξ in the frozen region. For $L \rightarrow \infty$ ξ_f/L diverges and thus, by increasing L , one has access to the whole FSS region. Thus, in the presence of freezing FSS can still be used but only in the form Eq. (13). Note that there is nothing special about our choice of ξ/L in Eq. (13), and indeed one can equally choose other RG invariant quantities, for instance the Binder cumulant, in the FSS analysis. Note that the presence of freezing and the limitations in the use of FSS are always expected in models with a $T=0$ transition and discrete Hamiltonian spectrum. In particular, these phenomena should also be considered in the three-dimensional (3D) diluted $\pm J$ Ising model close to the percolation point, where the glassy transition temperature vanishes [37].

Since ν does not appear in Eq. (13), this expression can only be used directly to check universality. If one is interested in computing ν , one must either work in infinite volume or use different FSS approaches. For instance, one can use the method proposed in Ref. [38] (Ref. [27] used it in this context), which relies on the finite-size behavior of ξ on lattices of size L and sL to obtain infinite volume estimates of ξ from which the exponent ν can be safely determined. In principle, one might also be able to use the methods of Ref. [39]. Note, however, that they rely on the behavior of the FSS functions close to the transition (i.e., for $\xi/L \rightarrow \infty$ or $U_4 \rightarrow 1$), which may not be accessible for reasonable lattice sizes due to the freezing.

C. Phenomenological couplings and universality

In order to verify universality, we consider the quartic cumulants U_4 and U_{22} , which should scale according to Eq. (13). The function $g_R(x)$ should be universal, hence p -independent. Universality is nicely supported by the data shown in Fig. 6. As expected, we find that $U_4 \rightarrow 3$ and $U_{22} \rightarrow 0$ for $\xi/L \rightarrow 0$, and $U_4 \rightarrow 1$ and $U_{22} \rightarrow 0$ for $\xi/L \rightarrow \infty$. All data for U_4 fall onto a single curve with small scaling corrections, supporting the existence of the finite-size scaling limit in terms of ξ/L , as discussed in the previous section. The convergence to a single curve is also clear in the case of U_{22} , although corrections are quite evident. Note that, in the region around the peak, for $\xi/L \approx 0.3$, the data at $p=4/5$ and $p=1/2$ converge from opposite sides.

In these universality checks there are no free parameters to be adjusted, and thus these comparisons provide strong support to the hypothesis that these models belong to the same universality class. Analogous universality checks for 2D Ising models with different distributions were performed in Refs. [27,28]. In Ref. [27], by studying the FSS behavior of $\xi(2L)/\xi(L)$ versus ξ/L , it was shown that several models with discrete distribution of the couplings are in the universality class of the $\pm J$ Ising model with $p=1/2$. In particular, universality was shown for the irrational model, a discrete model without energy gap which has the same stiffness ex-

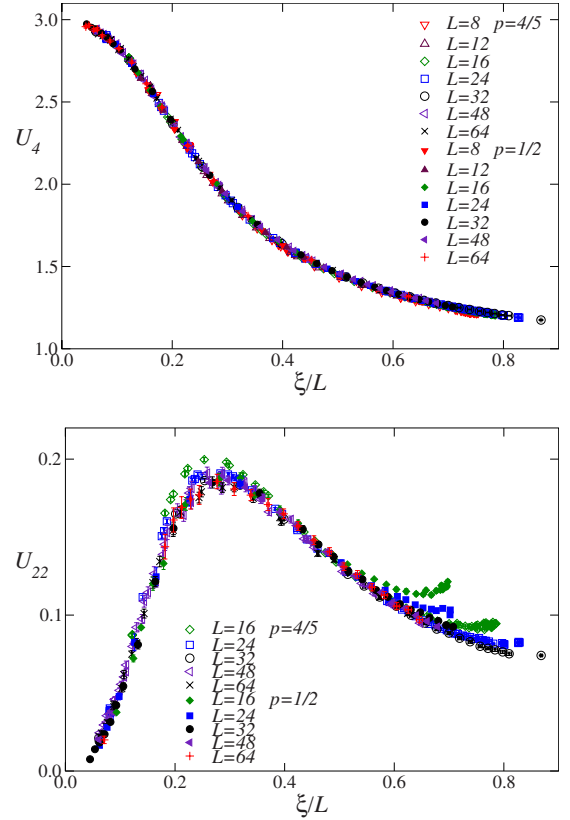


FIG. 6. (Color online) The quartic cumulants U_4 and U_{22} versus ξ/L for $p=4/5$ and $p=1/2$. We only plot data satisfying $L \geq 16$ for clarity.

ponent as continuous models [22]. Moreover, evidence of universality between the 2D Ising models with Gaussian and bimodal (our model with $p=1/2$) distributions was provided by the results of Ref. [28] for the FSS behavior of U_4 versus ξ/L .

We note that while the data for U_4 scale nicely up to $\xi/L \leq 0.9$, for U_{22} significant deviations are observed at smaller values of ξ/L , see Fig. 7. For $p=4/5$ and $L=8$ the data show significant deviations close to the peak, then approach the common curve and then show again a significant deviation—the data turn up—for $\xi/L > (\xi/L)_{\max} \approx 0.55$. A similar phenomenon occurs for $L=12$. For $L=16$ deviations close to the peak are quite small, but again the data begin to turn up as $\xi/L > (\xi/L)_{\max} \approx 0.6$. For $L=24$ FSS holds quite nicely, at least up to $(\xi/L)_{\max} \approx 0.65$. The value $(\xi/L)_{\max}$ marks the onset of the crossover region between the critical regime where FSS holds and the freezing regime that sets in at ξ_f/L . Note that ξ_f/L is significantly larger than $(\xi/L)_{\max}$, indicating that the breaking of FSS occurs much before freezing. For $p=1/2$ the conclusions are similar, although, for a given L , $(\xi/L)_{\max}$ is significantly smaller than the corresponding value for $p=4/5$. For instance, for $L=16$, we have $(\xi/L)_{\max} \approx 0.45$ for $p=1/2$ and $(\xi/L)_{\max} \approx 0.60$ for $p=4/5$. This clearly reflects the fact that ξ_f for $p=1/2$ is smaller than for $p=4/5$, see Fig. 5. Similar estimates of $(\xi/L)_{\max}$ for $p=1/2$ can be obtained from the results presented in Ref. [27].

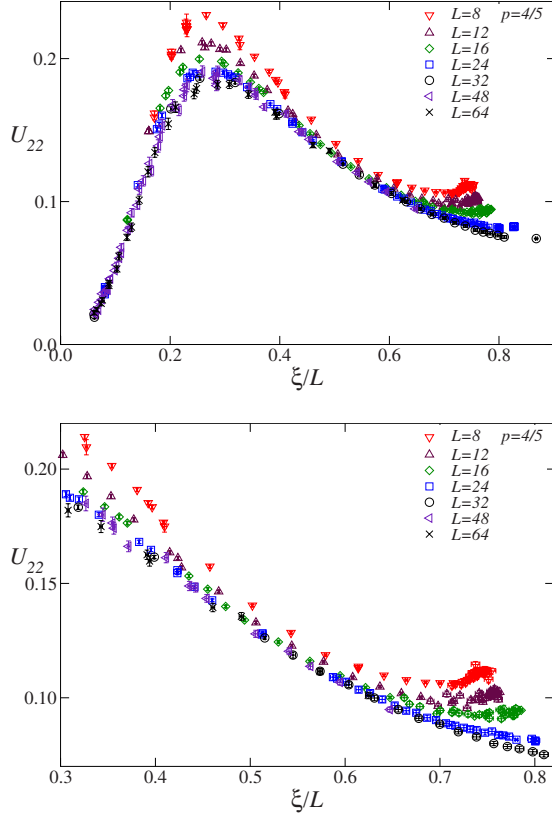


FIG. 7. (Color online) U_{22} versus ξ/L for $p=4/5$. We plot data for all available values of L . Below, we only show the results for $\xi/L > 0.3$.

D. Overlap susceptibility and exponent η

Finally, we investigated the critical behavior of the overlap susceptibility. As discussed in Ref. [33] it should behave in the FSS limit as

$$\chi = \bar{u}_h^2(T) L^{2-\eta} F_\chi(\xi/L), \quad (15)$$

where \bar{u}_h is an analytic function of T which is related to the overlap-magnetic scaling field. In order to determine η , we have performed fits of the data with $p=4/5$ to

$$\ln \chi = (2 - \eta) \ln L + P_n(T) + Q_m(\xi/L), \quad (16)$$

where $P_n(x)$ and $Q_m(x)$ are polynomials in x with $P_n(0)=0$. To avoid any bias from the presence of the freezing region, we have only used the data satisfying $\xi/L < (\xi/L)_{\max}$, where, for $L \leq 24$, $(\xi/L)_{\max}$ is the value determined before from the analysis of U_{22} . For $L=32$ we used somewhat arbitrarily $(\xi/L)_{\max}=0.7$, while for $L=48, 64$ we used all our data which in any case satisfy $\xi/L < 0.65$. To identify scaling corrections we only considered data satisfying $T < T_{\max}$ and $L > L_{\min}$ for several values of T_{\max} and L_{\min} . The results depend strongly on these parameters. For $T_{\max}=1.2$ we obtain $\eta=0.39(1)$ and $0.33(3)$ for $L_{\min}=8$ and 16 . For $L_{\min}=16$, we obtain $\eta=0.27(3)$, $0.24(3)$, and $0.22(4)$ for $T_{\max}=1$, 0.8 , and 0.6 . Apparently the results always decrease as T_{\max} decreases and L_{\min} increases. It is impossible to estimate reliably η from these results and, thus, we only quote an upper bound:

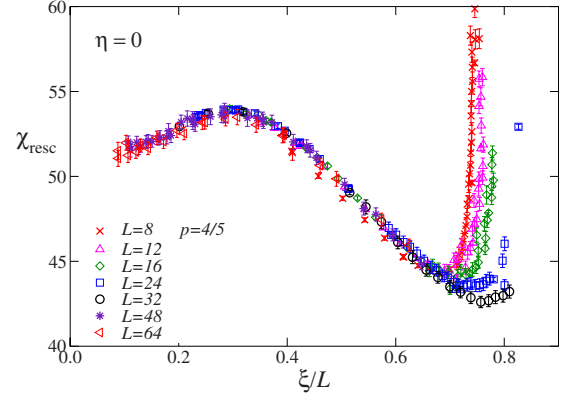


FIG. 8. (Color online) Rescaled susceptibility χ_{resc} defined in Eq. (18) for $p=4/5$ and $\eta=0$.

$$\eta \lesssim 0.2. \quad (17)$$

In principle, the same analysis can be performed for $p=1/2$. However, in this case the estimates of $(\xi/L)_{\max}$ are smaller, so that fewer data can be used in the fit. In practice, no estimates of η can be obtained.

As we mentioned at the beginning there are strong theoretical reasons to expect $\eta=0$. Thus, we tried to verify whether our results are consistent with this hypothesis. For this purpose we considered the data with $T_{\max}=1.0$ and $L_{\min}=12$ and we fitted them to Eq. (16) setting $\eta=0$. We find that the data satisfying $\xi/L < (\xi/L)_{\max}$ are reasonably described by Ansatz Eq. (15). In Fig. 8, we report

$$\chi_{\text{resc}} = \chi L^{-2} e^{-P_n(T)}, \quad (18)$$

where $P_n(T)$ is the polynomial determined in the fit Eq. (16). The agreement is quite good up to $(\xi/L) \approx 0.65$. It should be noted that, if we also include data with $\xi/L > (\xi/L)_{\max}$, the fits become much less dependent on T_{\max} and L_{\min} , exclude $\eta=0$, and give the estimate $\eta \approx 0.2$: Apparently the data that belong to the region $(\xi/L)_{\max} < \xi/L < \xi_f/L$ are well described by Eq. (15) with $\eta=0.2$, while they cannot be fitted by taking $\eta=0$. This is evident from Fig. 9 where we report $\chi L^{-1.8} \exp[-P_n(T)]$: in this figure essentially all data fall on a single rescaled curve. Note that the quality of the collapse is

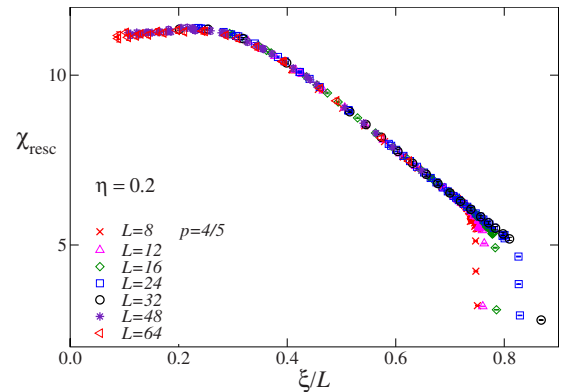


FIG. 9. (Color online) Rescaled susceptibility χ_{resc} defined in Eq. (18) for $p=4/5$ and $\eta=0.2$.

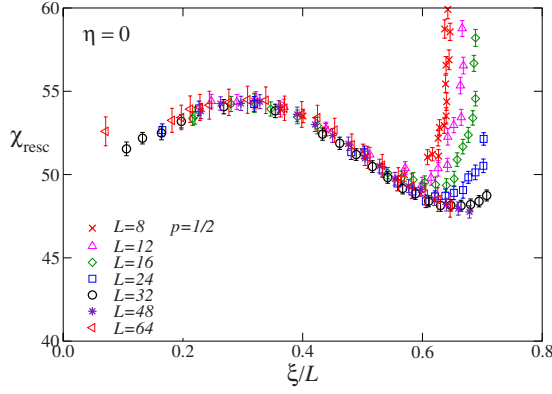


FIG. 10. (Color online) Rescaled susceptibility χ_{resc} defined in Eq. (18) for $p=1/2$ and $\eta=0$.

only marginally better than that given in Fig. 8—the χ^2 per degree of freedom of the fit is similar in the two cases—although this is not evident from the figures since they have a completely different vertical scale.

As a final check we verify if the data at $p=0.5$ are also consistent with $\eta=0$. The results are reported in Fig. 10. Also in this case the data with $\xi/L \leq 0.65$ are consistent with $\eta=0$. In the plot, we have also multiplied χ_{resc} by a constant in such a way that χ_{resc} assumes the value $\chi_{\text{resc}} \approx 56$ for $\xi/L \approx 0.3$ as it does for $p=4/5$. With this choice the curves for χ_{resc} should be the same for both values of p . As it can be seen the shape of the two curves is indeed the same. Quantitatively, the two curves are the same up to $\xi/L \approx 0.45$, while they differ significantly for $\xi/L \approx 0.6, 0.7$. This is not surprising. As we have explained, for $p=1/2$, the data such that $\xi/L \geq 0.5$ are probably already in the crossover region before the onset of freezing.

E. Magnetic quantities

The magnetic variables do not become critical in limit $T \rightarrow 0$. Indeed, the magnetic susceptibility χ_m and second moment correlation length ξ_m are finite in the limit $T \rightarrow 0$. For $p=1/2$ we have $\chi_m=1$ and $\xi_m=0$ for any T . For other values of p , they converge to nonuniversal values such that $\chi_m > 1$ and $\xi_m > 0$. For $p=4/5$ we find $\chi_m \approx 24$ and $\xi_m \approx 3.0$ in the limit $T \rightarrow 0$. We also consider the four-point magnetic susceptibility χ_{4m} which should scale as χ in the critical limit. In Fig. 11 we plot the ratio g_m/χ , where $g_m \equiv -\chi_{4m}/(\chi_m^2 \xi_m^2)$. This quantity shows smaller scaling corrections than χ_{4m}/χ and clearly converges to an L independent constant. The asymptotic behavior sets in for $T \lesssim 0.5$, before the freezing region $T \lesssim 0.35$.

IV. OVERLAP CRITICAL BEHAVIOR ALONG THE LOW-TEMPERATURE PARAMAGNETIC-FERROMAGNETIC TRANSITION LINE

We now investigate the behavior of the overlap correlations along the low-temperature PF transition line, see Fig. 1, from the MNP to the $T=0$ axis. The critical behavior of the magnetic correlations was numerically studied in Ref. [4] by varying p for two values of T : $T=1/1.55$ and $T=1/2$. It was

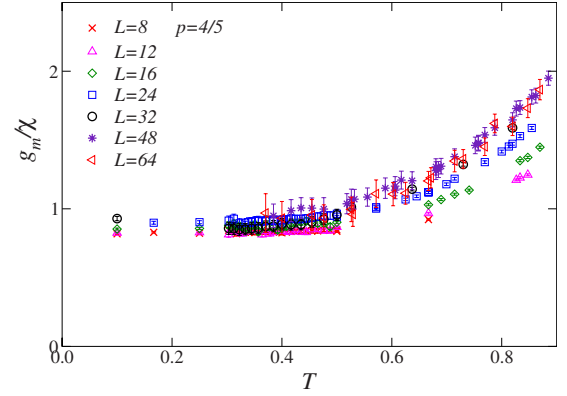


FIG. 11. (Color online) The ratio g_m/χ at $p=4/5$.

found that the critical behavior was universal, controlled by a single strong-disorder fixed point, with critical exponents $\nu \approx 3/2$ and $\eta_m \approx 1/8$.

The ferromagnetic $T=0$ transition point at $p=p_0 \approx 0.897$, where the low-temperature PF transition line ends, is a MGP, because it is connected to three phases and it is the intersection of two different transition lines, the PF line at $T>0$ and the glassy line at $T=0$. At $T=0$ the critical point at $p=p_0$ separates a ferromagnetic phase from a $T=0$ glassy phase, while for $T>0$ the transition line separates a ferromagnetic from a paramagnetic phase. Therefore, on general grounds, the critical behavior at $T=0$ and $p=p_0$ should differ from both that observed along the PF line and that observed along the glassy line $T=0$, $p>p_0$, unless the magnetic and glassy critical modes are effectively decoupled. Such a decoupling is apparently supported by the numerical results of Refs. [5,6,14,40]. Indeed, the estimates of the magnetic critical exponents at $T=0$ are quite close and substantially consistent with those found along the PF transition line below the MNP. All results are therefore consistent with a single magnetic fixed point that controls the magnetic critical behavior both at $T>0$ and at $T=0$. The analysis of the overlap correlation functions also supports the decoupling of the critical modes. Indeed, the arguments we gave in Sec. II on the behavior of the (overlap) phenomenological couplings and correlation functions should hold at $T=0$ for any value of p —hence, in the ferromagnetic phase, at the MGP as well as along the glassy transition line—since they only rely on the assumption of a nondegenerate ground state. Therefore, also at the $T=0$ MGP we expect $U_4=1$, $U_{22}=0$, $\xi/L=\infty$, and $\eta=0$. The behavior of the overlap correlations is therefore identical for $p>p_0$, for $p<p_0$, and at the MGP, in agreement with the decoupling scenario.

We wish now to understand the critical behavior of the overlap correlations along the PF line. In order to investigate this issue, we perform MC simulations at two critical points along the low-temperature PF line, at $[T=1/1.55 \approx 0.645, p=0.8915(2)]$ and $[T=1/2, p=0.8925(1)]$, as determined in Ref. [4], for lattice sizes up to $L=48$. The FSS analysis of the data of the overlap susceptibility χ shows that $\chi \sim L^{2-\eta}$ with quite small but nonzero values of η . Fits of the data satisfying $L \geq 16$ which take into account the nonanalytic scaling corrections give $\eta=0.046(6)$ at $T=1/1.55$ and $\eta=0.038(4)$ at $T=1/2$.

Note that these values are much smaller than the pure Ising value $\eta=1/2$ (which is simply twice the value of the magnetic exponent $\eta_m=1/4$) holding along the PF line from the pure Ising point to the MNP, and also much smaller than the value $\eta=\eta_m=0.177(2)$ at the MNP point. The FSS analyses of the phenomenological couplings ξ/L , U_4 and U_{22} lead to apparently T -dependent critical values: $U_{22}=0.018(2)$, $U_4=1.044(4)$, $\xi/L=1.7(1)$ at $T=1/1.55$, and $U_{22}=0.008(2)$, $U_4=1.025(2)$, and $\xi/L=2.2(1)$ at $T=1/2$ (where the errors are essentially due to the uncertainty on p_c and on the scaling correction exponent). Note that these values are very close to the values at the $T=0$ MGP; still we consider unlikely that the overlap behavior is the same as that occurring at the MGP, mainly because this would require $\xi/L=\infty$ along the whole PF line between the MNP and the MGP. Indeed, the condition $\xi/L=\infty$ is quite unlikely—we are not aware of systems in which this occurs—for a finite-temperature transition. These results can be better explained by a T -dependent asymptotic critical behavior which, with decreasing T , approaches the $T=0$ glassy behavior characterized by the values $\eta=0$, $U_{22}=0$, $U_4=1$, $\xi/L=\infty$.

V. CONCLUSIONS

In this paper we consider the two-dimensional $\pm J$ Ising model, focusing mainly on the $T=0$ glassy transition occurring for $1-p_0 < p < p_0$. The main results are the following:

(i) We first discuss the freezing phenomenon that occurs on any finite lattice at sufficiently low temperatures. We in-

vestigate the behavior of several quantities in this regime, verifying explicitly the expected logarithmic dependence on the lattice size L . We also show that the presence of this regime makes it impossible to use the standard form of FSS: the FSS limit $T \rightarrow 0$, $L \rightarrow \infty$ at fixed $TL^{1/\nu}$ does not exist. FSS can be formulated only if one considers ξ/L as basic FSS variable.

(ii) We study the FSS behavior of the quartic cumulants U_4 and U_{22} for $p=4/5$ and $p=1/2$ as a function of ξ/L . We find that they have the same FSS curves, a clear indication that the critical behavior for $p=4/5$ and $p=1/2$ is the same. This allows us to conjecture that the critical behavior is independent of p in the interval $1-p_0 < p < p_0$, and therefore, together with the results of Refs. [27,28], that there exists a single universality class for 2D Ising glassy transitions. We also investigate in detail the critical behavior of the overlap susceptibility, showing that the numerical data are consistent with $\eta=0$, if one discards data that are close to the region where freezing occurs.

(iii) Finally, we discuss the critical behavior of the overlap variables along the PF line. An analysis of the numerical data available for the $T=0$ MGP indicates that at this point glassy and magnetic modes are decoupled. For $T>0$ we observe an apparent T -dependent critical behavior. Note that a similar phenomenon was also observed in the XY model with random shifts [41]: along the critical line that starts at the XY pure point and ends at the Nishimori multicritical point, magnetic quantities show a universal behavior while overlap variables show a disorder-dependent critical behavior.

-
- [1] S. F. Edwards and P. W. Anderson, *J. Phys. F: Met. Phys.* **5**, 965 (1975).
 - [2] H. Nishimori, *Statistical Physics of Spin Glasses and Information Processing: An Introduction* (Oxford University Press, Oxford, 2001).
 - [3] N. Kawashima and H. Rieger, in *Frustrated Spin Systems*, edited by H. T. Diep (World Scientific, Singapore, 2004), 539; e-print [arXiv:cond-mat/0312432](https://arxiv.org/abs/cond-mat/0312432).
 - [4] F. Parisen Toldin, A. Pelissetto, and E. Vicari, *J. Stat. Phys.* **135**, 1039 (2009).
 - [5] C. Wang, J. Harrington, and J. Preskill, *Ann. Phys. (N.Y.)* **303**, 31 (2003).
 - [6] C. Amoruso and A. K. Hartmann, *Phys. Rev. B* **70**, 134425 (2004).
 - [7] H. Nishimori, *Prog. Theor. Phys.* **66**, 1169 (1981).
 - [8] The Nishimori line is defined by the equation $T=T_N(p)=2/[\ln p - \ln(1-p)]$. Along this line several rigorous results can be proved [2,7], such as the equality of the magnetic and overlap two-point correlations.
 - [9] H. Nishimori and K. Nemoto, *J. Phys. Soc. Jpn.* **71**, 1198 (2002).
 - [10] M. Ohzeki, *Phys. Rev. E* **79**, 021129 (2009).
 - [11] P. Le Doussal and A. B. Harris, *Phys. Rev. B* **40**, 9249 (1989); *Phys. Rev. Lett.* **61**, 625 (1988).
 - [12] M. Hasenbusch, F. Parisen Toldin, A. Pelissetto, and E. Vicari, *Phys. Rev. E* **77**, 051115 (2008).
 - [13] M. Hasenbusch, F. Parisen Toldin, A. Pelissetto, and E. Vicari, *Phys. Rev. E* **78**, 011110 (2008).
 - [14] W. L. McMillan, *Phys. Rev. B* **29**, 4026 (1984).
 - [15] The presence of two different universality classes along the paramagnetic-ferromagnetic transition line is neither peculiar of the $\pm J$ model nor is it restricted to two dimensions. For instance, approximate RG calculations suggest that a similar phenomenon occurs in the three-dimensional Blume-Emery-Griffiths model with bond randomness [A. Falicov and A. N. Berker, *Phys. Rev. Lett.* **76**, 4380 (1996)].
 - [16] G. Migliorini and A. N. Berker, *Phys. Rev. B* **57**, 426 (1998).
 - [17] H. Rieger, L. Santen, U. Blasum, M. Diehl, M. Jünger, and G. Rinaldi, *J. Phys. A* **29**, 3939 (1996); **30**, 8795(E) (1997).
 - [18] J. Houdayer, *Eur. Phys. J. B* **22**, 479 (2001).
 - [19] In the parallel-tempering runs, we divided the interval between T_{\min} and T_{\max} in N_T-1 intervals chosen so that the exchange acceptance between adjacent temperatures is roughly constant. Typically we had: $N_T=3$ for $L=8$, $N_T=3-4$ for $L=12$, $N_T=4-5$ for $L=16$, $N_T=8$ for $L=24$, $N_T=12$ and 26 for $L=32$, $N_T=9, 10, 11$, and 33 for $L=48$, and $N_T=12, 14$, and 33 for $L=64$.
 - [20] A. K. Hartmann and A. P. Young, *Phys. Rev. B* **64**, 180404(R) (2001).
 - [21] A. C. Carter, A. J. Bray, and M. A. Moore, *Phys. Rev. Lett.* **88**, 077201 (2002).
 - [22] C. Amoruso, E. Marinari, O. C. Martin, and A. Pagnani, *Phys.*

- Rev. Lett.* **91**, 087201 (2003).
- [23] J. Lukic, A. Galluccio, E. Marinari, O. C. Martin, and G. Rinaldi, *Phys. Rev. Lett.* **92**, 117202 (2004).
- [24] J. Houdayer and A. K. Hartman, *Phys. Rev. B* **70**, 014418 (2004).
- [25] H. G. Katzgraber, L. W. Lee, and A. P. Young, *Phys. Rev. B* **70**, 014417 (2004).
- [26] H. G. Katzgraber and L. W. Lee, *Phys. Rev. B* **71**, 134404 (2005).
- [27] T. Jörg, J. Lukic, E. Marinari, and O. C. Martin, *Phys. Rev. Lett.* **96**, 237205 (2006).
- [28] H. G. Katzgraber, L. W. Lee, and I. A. Campbell, *Phys. Rev. B* **75**, 014412 (2007).
- [29] A. K. Hartmann, *Phys. Rev. B* **77**, 144418 (2008).
- [30] M. Ohzeki and H. Nishimori, *J. Phys. A: Math. Theor.* **42**, 332001 (2009).
- [31] The most accurate estimates of ν have been obtained by computing the stiffness exponent $\theta = -1/\nu$ at $T=0$ in models with continuous distributions. We mention $\theta = -0.281(2)$ (Ref. [17]), $\theta = -0.282(2)$ (Ref. [20]), $\theta = -0.282(3)$ (Ref. [21]), and $\theta = -0.282(4)$ (Ref. [22]) obtained by using the Ising glass model with a Gaussian distribution for the couplings, and $\theta = -0.275(5)$ [F. Liers, J. Lukic, E. Marinari, A. Pelissetto, and E. Vicari, *Phys. Rev. B* **76**, 174423 (2007)] obtained in the random-anisotropy model in the strong-anisotropy limit, whose glassy critical behavior is in the same universality class.
- The stiffness exponent is instead not related to ν in the case of discrete distributions with quantized Hamiltonian spectrum [22,27]. Finite-temperature estimates of ν are reported in Refs. [24,25,27,28].
- [32] G. Toulouse, *J. Phys. Lett.* **41**, 447 (1980).
- [33] M. Hasenbusch, A. Pelissetto, and E. Vicari, *Phys. Rev. B* **78**, 214205 (2008); *J. Stat. Mech.: Theory Exp.* (2008), L02001.
- [34] J. W. Landry and S. N. Coppersmith, *Phys. Rev. B* **65**, 134404 (2002).
- [35] K. Binder and A. P. Young, *Rev. Mod. Phys.* **58**, 801 (1986).
- [36] C. J. Geyer, in *Computer Science and Statistics*, Proceedings of the 23rd Symposium on the Interface, edited by E. M. Keramidas (Interface Foundation, Fairfax Station, 1991), p. 156; K. Hukushima and K. Nemoto, *J. Phys. Soc. Jpn.* **65**, 1604 (1996); D. J. Earl and M. W. Deem, *Phys. Chem. Chem. Phys.* **7**, 3910 (2005).
- [37] T. Jörg and F. Ricci-Tersenghi, *Phys. Rev. Lett.* **100**, 177203 (2008).
- [38] S. Caracciolo, R. G. Edwards, S. J. Ferreira, A. Pelissetto, and A. D. Sokal, *Phys. Rev. Lett.* **74**, 2969 (1995).
- [39] T. Jörg and H. G. Katzgraber, *Phys. Rev. Lett.* **101**, 197205 (2008).
- [40] M. Picco, A. Honecker, and P. Pujol, *J. Stat. Mech.: Theory Exp.* (2006), P09006.
- [41] V. Alba, A. Pelissetto, and E. Vicari, *J. Stat. Mech.: Theory Exp.* (2010), P03006.